Rapid Infarct Imaging with a Technetium-99m-Labeled Antimyosin Recombinant Single-Chain Fv: Evaluation in a Canine Model of Acute Myocardial Infarction

Mark A. Nedelman, David J. Shealy, Raymond Boulin, Eva Brunt, Julia I. Seasholtz, I. Elaine Allen, John E. McCartney, Frederick D. Warren, Herman Oppermann, Roy H. L. Pang, Harvey J. Berger and Harlan F. Weisman

Research and Development Division of Centocor, Inc., Malvern, Pennsylvania and Creative Biomolecules, Hopkinton, Massachusetts

Studies of monoclonal antibody-based imaging agents show that blood clearance is inversely proportional to molecular size, i.e., Fab or Fab' > F(ab')₂ > IgG. Indium-111-antimyosin Fab-DTPA is a highly specific and sensitive marker for myocardial necrosis. An improvement on current antibody diagnostic imaging may result from the use of smaller labeled fragments. We report the first in vivo targeting of acute myocardial infarction with a novel recombinant single-chain Fv (sFv) antimyosin protein. The sFv (MW = 27,594) is approximately one-half the size of the Fab and is comprised of the heavy and light chain variable regions from the myosin-specific murine monoclonal antibody R11D10 which were joined by a 15-amino-acid linker and expressed as a fusion protein (sFv) in E. coli. The binding affinity of the sFv for cardiac myosin was similar to the affinity observed for the Fab fragment. Technetium-99m labeling of the sFv was accomplished by the attachment of a cleavable, ester-linked bifunctional chelator (RP-1). Comparative studies in mice showed ^{99m}Tc-sFv-RP-1 cleared significantly faster (p < 0.001) than ^{99m}Tc-Fab'-RP-1 and ^{111}In-Fab-DTPA antimyosin fragments. Furthermore, measurement of ^{99m}Tc-sFv-RP-1 blood clearance in a canine model of acute myocardial infarction gave a mean $T_{1/2}$ of 0.54 ± 0.13 hr versus 2.80 ± 0.57 and 2.58 ± 0.64 hr for Fab-DTPA and Fab'-RP-1 (p < 0.05), respectively. Despite its comparatively rapid clearance, ^{99m}Tc sFv-RP-1 had similar uptake in the infarct compared to the Fab'-RP-1. In addition, infarct visualization was more rapid with the sFv. Thus, these data demonstrate antimyosin sFv possesses characteristics necessary for rapid imaging of myocardial necrosis.

J Nucl Med 1993; 34:234–241

$\mathbf{T}$he generation of a diagnostic image requires that sufficient contrast (target-to-background) is achieved. Fol-

lowing intravenous administration of imaging agents, more rapid images could be obtained if augmented clearance of activity from blood or nontarget related activity was achieved. Studies of monoclonal antibody (Mab) based imaging agents have shown that blood clearance is inversely related to the size of the injected protein, i.e., Fab or Fab' > F(ab')₂ > IgG (1,2). In addition to faster blood clearance, Mab fragments have advantages over the whole Mab by reducing the immunogenic potential, because the Fc portion of the Mab is removed (3,4). However, these Mab fragments are advantageous only if they retain sufficient affinity or uptake at the target.

Indium-111-antimyosin Fab-DTPA is a highly sensitive and specific marker for the detection of the presence, location and extent of myocardial necrosis (5,6). Diagnostic images with antimyosin Fab-DTPA are often delayed because of its relatively slow blood clearance. Although methods have recently been developed to rapidly and quantitatively label proteins with ^{99m}Tc (the radionuclide of choice in nuclear medicine), there is a clinical need to increase blood clearance further.

Recent technology development has made possible the generation of recombinant/chimeric genes and "designer" proteins. Specifically, single-chain antibodies, or single-chain Fv (sFv) proteins, have been developed (7–9). These sFvs are composed of the variable heavy-chain sequence (V$_H$) tethered or joined to the variable light-chain sequence (V$_L$) and are approximately one-half the molecular weight of the Fab fragment (27 versus 50 kdaltons). An antimyosin single-chain sFv was constructed and expressed in E. coli as a fusion protein (sFv) and shown to have similar affinity for myosin as that of the Fab fragment. In addition, ^{99m}Tc labeling was accomplished by attachment of a cleavable, ester-linked bifunctional chelator (RP-1). We report the in vivo evaluation of this ^{99m}Tc-labeled antimyosin sFv fragment. Biodistribution of ^{99m}Tc-sFv-RP-1 in mice, as well as the pharmacokinetics and imaging properties in a canine model of acute myocardial infarction were evalu-

ated and compared to ^{99m}Tc-Fab'-RP-1 and ^{111}In Fab-DTPA antimyosin.

MATERIALS AND METHODS

Cloning, Construction and Expression of the Antimyosin sFv

The cloning of the heavy- and light-chain DNA sequences, as well as construction and expression of the sFv followed the procedures detailed previously (7). Briefly, polyadenylated RNA was isolated from approximately 1×10^8 R11D10 hybridoma cells using a mRNA isolation kit (Invitrogen Fast Track). A cDNA library was constructed with 2 μg of the isolated mRNA using the lambda ZAPII cloning vector. The heavy- and light-chain sequences were isolated by screening this library with probes coding for the four heavy-chain J segments and the five kappa light-chain J regions, respectively. The N-terminal amino acid sequences predicted by the DNA sequences of the isolated heavy and light chains were identical to those of the purified immunoglobulin secreted by R11D10 hybridoma cells.

Boundaries for the heavy- and light-chain variable region domains were determined by comparison of the cloned sequences to known sequences for the J segments and other mouse immunoglobulins. The sFv was constructed in the order V_H-V_L, connected with a 15-amino acid linker (gly-gly-gly-gly-ser)$_3$. The protein was expressed in $E.\ coli$ under the control of trp promoter as a fusion protein with a 15-amino-acid leader sequence (sL). The expression level of the sFv was estimated to be about 30% of the total cellular protein.

Isolation of Antimyosin sFv

Following fermentation, bacterial cells were disrupted by a French press and the inclusion bodies collected by centrifugation. The protein was solubilized by resuspending the inclusion bodies in 25 mM Tris pH 8.2, 10 mM EDTA, 250 mM 2-mercaptoethanol, 7 M guanidine-HCl. After diluting the protein to an A280 of 0.2 in 25 mM Tris pH 8.6, 10 mM EDTA, 4 M guanidine HCl, 1 mM oxidized glutathione, 0.1 mM reduced glutathione, the sFv was allowed to oxidize overnight at room temperature and then refolded by extensive dialysis against 10 mM sodium phosphate, 1 mM EDTA, 0.5 M urea, pH 8.0. The refolded sFv preparation was passed through a DE52 (Whatman) column and purified to homogeneity using a myosin affinity column.

Preparation of Antimyosin sFv-RP-1

Preparation and characterization of the RP-1 chelator was as previously described (10). Purified sFv was dialyzed into buffer A (10 mM sodium phosphate pH 7.0, 10 mM NaCl, 0.5 M urea, 1 mM EDTA). Free thiols were inserted by adding 0.25 volume of 0.3 M triethanolamine pH 8.0, 5 mM EDTA and 0.01 volume of 0.5 M 2-iminothiolane in buffer A and incubating for 1–2 hr on ice. After redialyzing into buffer A, the number of free thiols present were assayed using Ellman's reagent (11). A tenfold molar excess of RP-1 over free thiols was added in 0.10 volume 60% ethanol, 40% buffer A, and the mixture was incubated for 60 min on ice. The sample was again dialyzed into buffer A, and concentrated to approximately 0.30 mg/ml. To the protein conjugate was added 0.1 volume of 100 mM dithiothreitol to remove the isophthaloyl protecting group on RP-1. After incubation for 1 hr at room temperature, the sample was dialyzed into buffer A. An aliquot of the final product, sFv-RP-1, was blocked with N-ethylmaleimide to prevent oxidative dimerization and assayed

for binding affinity for canine heart myosin using an ELISA plate assay.

Aliquots of the labeled protein solution were analyzed for unbound ^{99m}Tc by instant thin-layer chromatography (ITLC) on silica-gel impregnated glass fiber sheets (Gelman Sciences) using 0.1 M citrate pH 5.0 and water:ethanol:ammonium hydroxide (365:121:1) as the developing solvents. Free ^{99m}TcO$_4^-$ ranged from 4% to 8% and ^{99m}TcO$_2\cdot$nH$_2$O colloids from 0.8% to 1.4%.

Preparation of Dog Heart Myosin and Myosin-Sepharose. Dog heart myosin was prepared from the left ventricle and septum as previously described (12). The purity of the dog heart myosin was confirmed by SDS-gel electrophoresis and stored at $-20°$C in 5 mM 3-(N-morpholino)propanesulfonic acid (MOPS), 2.5 mM [ethylene-bis(oxyethylene-nitro)]tetraacetic acid (EGTA), 0.5 mM dithiothreitol, 0.3 M sodium chloride, 50% (v/v) glycerol pH 7.5. Myosin-Sepharose was prepared using cyanogen bromide-activated Sepharose CL-4B (Millipore) as described in the manufacturer's instructions. The efficiency of coupling was typically greater than 90%.

Determination of Immunoreactivity

Myosin-Sepharose Immunoreactivity Assay. Technetium-99m antimyosin fragments were diluted 1:10 in phosphate-buffered saline (PBS)1% BSA and 100 μl was applied to a 1-ml column of myosin-Sepharose. The column was washed with 10 ml of PBS-1% bovine serum albumin (BSA) and eluted with 10 ml of 0.1 M glycine pH 2.5. One milliliter aliquots of these two fractions were counted in a gamma counter set for ^{99m}Tc, as well as an aliquot of the sample applied to the column. Total recovery of ^{99m}Tc from the column ranged from 91% to 99%. The percent of ^{99m}Tc eluting with the glycine buffer was divided by the total ^{99m}Tc recovered from the column to determine the percent immunoreactivity.

Competitive ELISA Immunoreactivity Assay. Polyvinylchloride 96-well microtiter plates were coated with dog heart myosin at a concentration of 100 μg/ml, 75 μl per well in 0.06 M Tris pH 6.8, 0.75 M KCl, 0.02 M sodium azide overnight at room temperature. Wells were washed in the same buffer, blocked with 150 μl per well of PBS-1% BSA for 1 hr at room temperature, and then blotted dry. Ten threefold serial dilutions of each sample were prepared in PBS-1% BSA beginning with an initial protein concentration of 0.05 mg/ml. An equal volume of alkaline phosphatase-conjugated antimyosin IgG, diluted 1:1000 in PBS-1% BSA, was added to each serial dilution. Each dilution was then dispensed (75 μl per well) in duplicate and incubated on the myosin-coated plate for 5 hr at room temperature. Plates were washed three times in PBS-0.05% Tween 20, and a substrate solution was prepared by dissolving one tablet of p-nitrophenyl phosphate (Sigma) per 5 ml of 2-amino-2-methyl-1-propanol buffer (Sigma) diluted 500-fold in distilled water. The substrate solution was dispensed (100 μl per well), the plates covered with aluminum foil and incubated for 30 min in a 37°C water bath. Color development was stopped by adding 50 μl of 3 M NaOH to each well and absorbance at 405 nm was read within 1 hr. The log (pmoles/ml) protein concentration was plotted against the average absorbance at 405 nm. The protein concentration at 50% inhibition was determined from the graph using a four-parameter fit.

Technetium-99m Labeling

An aliquot of the sFv-RP-1 chelator conjugate (0.5 mg/2.0 ml) was labeled with ^{99m}Tc (25 mCi, ^{99}Mo/^{99m}Tc generator eluent) as

described previously (*10*). An aliquot of the ^{99m}Tc-labeled conjugate was loaded onto a myosin-sepharose affinity column to test for immunoreactivity, resulting in 86% binding with 94% recovery.

Biodistribution Studies

Biodistribution studies were conducted in normal CF-1 female mice (Charles River, Wilmington, MA) 6–8 wk of age. Approximately 100 μCi/5.0 μg of ^{99m}Tc sFv-RP-1 in 0.1 ml of saline was administered intravenously via a lateral tail vein. Mice were killed by cervical dislocation, organs excised, weighed and studied for biodistribution at 0.25, 1.0, 2.0, 5.0 and 24 hr employing a multichannel gamma scintillation counter (LKB, Model 1282) set to detect the 143 keV photopeak of ^{99m}Tc. The percentage of the injected dose per gram of tissue (%ID/g) was determined for blood, heart, lung, liver, spleen, kidneys, stomach, small intestine, large intestine, ovaries and muscle at each of the time points (four mice per time point). Comparative biodistribution studies were performed for ^{111}In-Fab-DTPA and ^{99m}Tc-Fab'-RP-1 antimyosin in an identical fashion.

Experimental Model

A standard model of acute myocardial infarction was employed (*13*). Briefly, 15–20-kg dogs were anesthetized with intravenous sodium pentobarbital (30 mg/kg), intubated and ventilated on room air. Peripheral lines were placed for administration of test agents and drugs as well as blood sampling. All blood samples were collected from a site distant from that used for administration of radiolabeled agents. A left thoracotomy was performed at the 5th intercostal space exposing the heart. Once suspended in a pericardial cradle, the left anterior descending (LAD) branch of the coronary artery was isolated by blunt dissection distal to the first diagonal branch. A silk ligature was used to snare the LAD. An occlusion/reperfusion protocol was employed to produce myocardial infarcts. Flow in the LAD was occluded by constriction of the ligature for approximately 2 hr followed by reperfusion. Fifteen minutes after reperfusion, test agents were injected intravenously.

Two complementary sets of experiments were performed to facilitate the evaluation of the in vivo characteristics of the ^{99m}Tc-sFv-RP-1. In the first, both ^{99m}Tc-sFv-RP-1 (20 mCi/0.5 mg) and ^{111}In-Fab-DTPA (2.0 mCi/0.5 mg) were administered simultaneously to permit direct comparison of the sFv and Fab-DTPA in the same animal (n = 4). In a second set of studies, the same protocol was employed, utilizing ^{99m}Tc-Fab'-RP-1 and ^{111}In-Fab-DTPA (n = 4). This permitted comparison of the sFv results from the first set of studies with the Fab' results from the second set of studies, using the identical radioisotope and chelator, albeit in different animals.

Venous blood samples were obtained at 1, 5, 10, 15, 30, 60, 120, 180, 260 and 300 min after intravenous administration of the antimyosin fragments for analysis of blood clearance. The radioactivity in the 1-min blood sample was used as the 100% activity value for calculating blood clearance rates. Serial gamma images were acquired hourly for 5 hr for both the sFv or Fab' (pulse height analyzer set to detect the 143 keV photopeak of ^{99m}Tc, 20% window) and Fab-DTPA (set only to detect the 247 keV photopeak of ^{111}In, 20% window). Following the end of the in vivo portion of the protocol, animals were killed by anesthesia overdose and infusion of 2% triphenyltetrazolium chloride (TTC, Sigma Chemical Co., St. Louis, MO). Histochemical delineation by TTC was employed in all studies to confirm acute myocardial

infarction. The hearts were excised, rinsed of residual blood and sliced transversely in 1–2 cm sections parallel to the atrioventricular groove from base to apex. Each serial section then was imaged. After imaging, the heart slices were mapped and cut into approximately 1-g pieces separating endo- and epicardial myocardium when possible, weighed and then counted for radioactivity. Uptake ratios for antimyosin were generated by comparing activity in the infarct to that in normal myocardium. Endocardial samples from the basal-most slice were chosen as normal, since these myocardial samples were clearly proximal to the LAD occlusion.

Data Analysis

Statistical comparisons of sFv-RP-1 with Fab'-RP-1 and Fab-DTPA were performed using analysis of variance. Tukey's studentized range test (*14*) was used for multiple comparisons. All analyses were based on a two-sided alternative, and differences were considered to be significant if p ≤ 0.05.

A one-compartment model of the form

$$Y = ae^{-\alpha t}$$

was fit to data for radioactivity remaining in the blood using SAS PROC NLIN (*15*), using a Marquardt algorithm for minimizing the residuals of the least squares fit. Parameters estimated included volume of distribution, elimination rate, 24-hr concentration, and mean half-life ($T_{1/2}$). The mean fitted parameters of each model were compared using an analysis of variance with multiple comparison testing as indicated above.

RESULTS

Immunoreactivity of the antimyosin sFv and sFv-RP-1 conjugate were compared to antimyosin Fab-DTPA using a competitive binding ELISA. This assay measures the ability of the test sample to compete with alkaline phosphatase-conjugated antimyosin IgG for binding to a myosin-coated microtiter plate. The resulting titration curves (Fig. 1) were nearly identical, indicating that there were
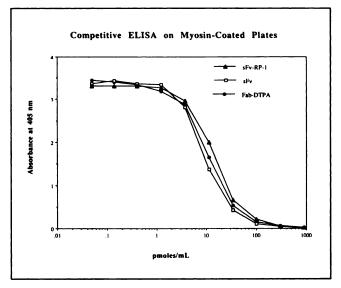

FIGURE 1. Immunoreactivity of the antimyosin sFv and sFv-RP-1 conjugate were compared to the Fab-DTPA using a competitive binding ELISA. Preparation of the sFv and subsequent conjugation with the RP-1 ligand employed in the in vivo evaluations, had no effect on the myosin binding site.
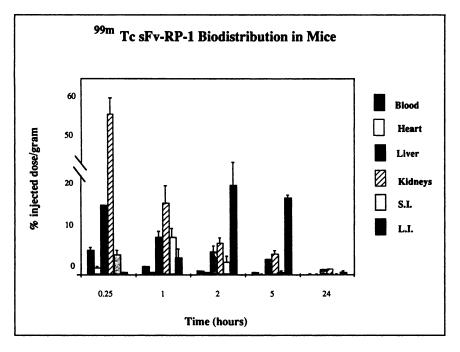
FIGURE 2. Biodistribution of ^{99m}Tc antimyosin sFv-RP-1 in mice. Each animal was injected intravenously with 100 μCi/5 μg in a volume of 0.1 cc. Data are shown as % ID/g of tissue and represent the mean and s.d. for four mice at each time point. (S.I. = small intestine and L.I. = large intestine).

no significant differences between the three samples. This result confirms that the preparation of the sFv and subsequent conjugation with RP-1 had no effect on the myosin binding site. The molar concentrations of each fragment which resulted in 50% inhibition were 10.6 nM for Fab-DTPA, 8.9 nM for sFv and 14.0 nM for sFv-RP-1.

Biodistribution

A biodistribution study was performed in mice to evaluate the blood clearance of ^{99m}Tc sFv-RP-1, as well as its whole-body distribution. The biodistribution of ^{99m}Tc sFv-RP-1 in mice is illustrated in Figure 2. Blood clearance of the sFv was extremely rapid with only 5.7 ± 0.7 %ID/g remaining in the blood 15 min after intravenous administration. The majority of radioactivity at 15 min after administration (54.3 ± 4.9 %ID/g) was localized in the kidneys, the major route of excretion. Radioactivity decreased over time in all organs studied except for the gastrointestinal tract. With both ^{99m}Tc RP-1 labeled fragments, activity accumulated in the small and then large intestine in the first 2 to 5 hr, but were almost completely eliminated by 24 hr. The result was expected because the RP-1 chelator is believed to be metabolized and cleared via the hepatobiliary system (10).

Figure 3 illustrates comparative blood levels in mice at 2 and 24 hr after intravenous injection of ^{99m}Tc-sFv-RP-1, ^{99m}Tc-Fab'-RP-1 and ^{111}In-Fab-DTPA antimyosin fragments. Blood levels at 2 and 24 hr were comparable for ^{111}In-Fab-DTPA and ^{99m}Tc-Fab'-RP-1. By contrast, ^{99m}Tc-sFv-RP-1 blood levels were significantly (p < 0.001) lower at both 2 and 24 hr compared to both ^{99m}Tc-Fab'-RP-1 and ^{111}In-Fab-DTPA antimyosin fragments. These results prompted additional studies in a canine model of acute myocardial infarction to better evaluate the clearance ki-

netics and imaging properties of the three labeled fragments.

Infarct Studies

Figure 4 illustrates blood clearance curves in dogs for each of the fragments. Similar to the results in mice, clearance of ^{99m}Tc-Fab'-RP-1 and ^{111}In-Fab-DTPA from the blood were equivalent. However, clearance of ^{99m}Tc-sFv-RP-1 from the blood was 4 to 5 times faster than
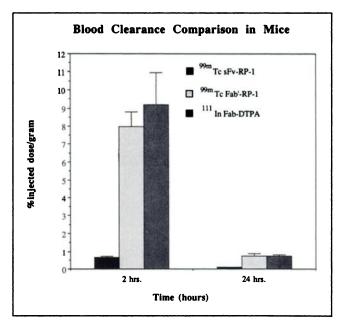

FIGURE 3. Comparative blood levels in mice for ^{99m}Tc-sFv-RP-1, ^{99m}Tc-Fab'-RP-1 and ^{111}In-Fab-DTPA antimyosin fragments at 2 and 24 hr. The ^{99m}Tc-sFv-RP-1 exhibited significantly (p < 0.001) lower blood levels at both time points. Data represent mean ± s.d. for four animals per time point.
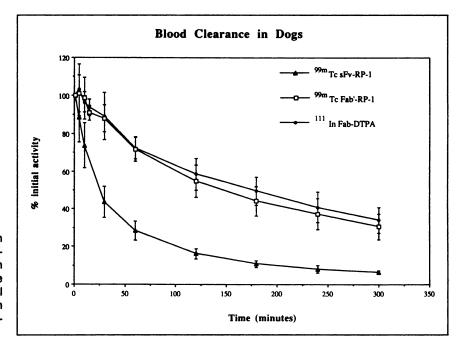
Blood Clearance in Dogs

FIGURE 4. Blood clearance curves in dog for ^{99m}Tc-sFv-RP-1 (n = 5), ^{99m}Tc-Fab'-RP-1 (n = 5) and ^{111}In-Fab-DTPA (n = 8) antimyosin fragments. The data are presented as the percentage of the initial activity (mean ± s.d.) assuming the 1-min blood sample represents 100% of the injected activity.

either ^{99m}Tc-Fab'-RP-1 or ^{111}In-Fab-DTPA. A summary of the pharmacokinetic parameters evaluated for each fragment is shown in Table 1.

Comparative scintigraphic studies were conducted for the evaluation of infarct visualization by each fragment. Figure 5 shows serial left lateral images at 1, 3 and 5 hr after administration of ^{99m}Tc-Fab'-RP-1 and ^{111}In-Fab-DTPA in a representative study. The 1-hr images show blood-pool activity enabling visualization of the right and left ventricle. By 3 hr postadministration of both radiolabeled fragments, unequivocal uptake of activity is evident in the anteroapical region of the heart which corresponded to the site of infarction. Contrast for both ^{99m}Tc-Fab'-RP-

TABLE 1
Summary of Pharmacokinetic Parameters of Antimyosin Fragments in Dogs

Fragment	24-hr concentration (μCi/ml)	Clearance rate (ml/kg/hr)	Volume of distribution (ml/kg)	Half-life (hr)
Fab-DTPA				
mean	7.82	12.67	49.44	2.80
s.d.	9.86	2.74	3.31	0.57
Fab'-RP-1				
mean	51.97	13.95	50.03	2.58
s.d.	69.61	3.18	2.92	0.64
sFv-RP-1				
mean	<0.01*	68.67*	20.27	0.54*
s.d.	<0.01	17.30	3.20	0.13

* $p < 0.05$ versus Fab-DTPA and Fab'-RP-1.

A one-compartment model was fit to the data for radioactivity (mCi) remaining in the blood. Data were generated by using the 1-min blood sample as 100% of the injected activity [2 mCi for Fab-DTPA (n = 8) and 20 mCi for Fab'-RP-1 (n = 4) and sFv-RP-1 (n = 4)].

1 and ^{111}In-Fab-DTPA increased over time as radioactivity cleared from the blood, but blood-pool activity remained for both radiolabeled preparations at 5-hr postinjection. In contrast to ^{111}In-Fab-DTPA, which is excreted primarily by the kidneys, a significant portion of ^{99m}Tc is cleared by the hepatobiliary system as shown by the accumulation of activity in the gallbladder in the 3- and 5-hr Fab'-RP-1 images. This is consistent with biodistribution studies for other ^{99m}Tc-labeled antibody fragments utilizing the RP-1 chelator (data not shown).

Figure 6 illustrates a representative set of images for ^{99m}Tc-sFv-RP-1. Within 1 hr of administration of sFv, there was unequivocal visualization of the infarct. Blood-pool activity was dramatically reduced by 1 to 3 hr, allowing further delineation of the infarct. Analysis of the 5-hr images revealed minimal cardiac blood-pool activity as reflected in the significantly lower blood levels for the sFv (6.3 ± 0.3% of the initial activity) compared to those for the ^{99m}Tc-Fab'-RP-1 (30.4 ± 6.9%) and ^{111}In-Fab-DTPA (34.0 ± 6.9%) (Fig. 4). Infarct size was similar to that found in Figure 5. Similar to the ^{99m}Tc-Fab'-RP-1, the ^{99m}Tc-sFv-RP-1 exhibited both renal and hepatobiliary clearance.

Table 2 summarizes infarct uptake at 5 hr for the antimyosin fragments. Infarct uptake of Fab'-RP-1 and Fab-DTPA was similar as measured by infarct-to-normal and infarct-to-blood ratios. However, sFv-RP-1 had markedly greater infarct uptake as measured by these indices. No significant difference was observed between any of the fragments for absolute uptake (%ID/g) at the infarct.

DISCUSSION

Since the original description of antimyosin IgG (14), numerous advances have been made in both the radiolabel and antibody fragment used. Previous studies with anti-
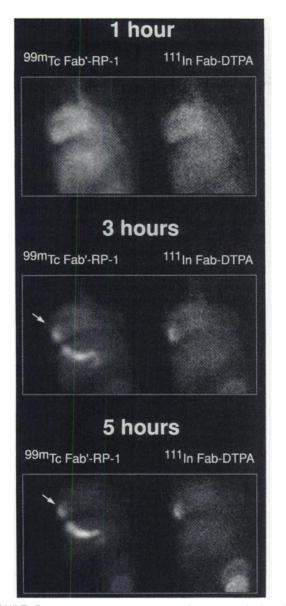
FIGURE 5. Comparative scintigrams from a study in which ^{99m}Tc-Fab'-RP-1 (20 mCi/0.5 mg) and ^{111}In-Fab-DTPA (2 mCi/0.5 mg) antimyosin were coadministered. Serial images (left lateral view) illustrate equivalent uptake in the infarct (shown by the arrow) for both tracers. All images were normalized to the 1-hour image. Significant ^{99m}Tc activity in the gallbladder is evident in the later images for the Fab'-RP-1 due to the hepatobiliary excretion of the RP-1 chelate. Blood clearance and infarct localization for ^{99m}Tc-Fab'-RP-1 and ^{111}In-Fab-DTPA showed no significant differences.

FIGURE 6. Representative images from a study with ^{99m}Tc-sFv-RP-1 (20 mCi/0.5 mg). Serial left lateral images show initial blood-pool images. Unequivocal infarct visualization is evident by 1 hour with the sFv-RP-1 (arrow). Cardiac blood background is cleared significantly faster for the sFv-RP-1 than either the Fab-DTPA or Fab'-RP-1. All images were normalized to activity in the initial image. Similar to the Fab'-RP-1, activity accumulates in the hepatobiliary tree over time as the RP-1 chelate is excreted.

myosin-based imaging agents have employed either polyclonal or monoclonal antibodies produced by hybridoma technology in generating antibodies and the subsequent fragments directed against cardiac myosin. The present study describes a single-chain antibody molecule, ^{99m}Tc-labeled antimyosin sFv fragment, produced by genetic and protein engineering for imaging myocardial necrosis.

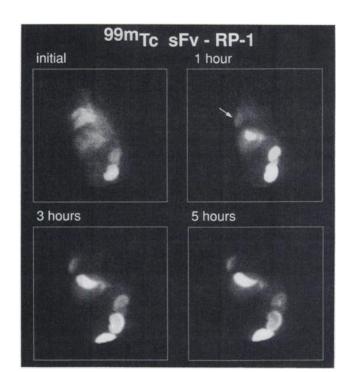High background has been a persistent problem with imaging agents using intact antibody molecules. Improvements in the rate of blood clearance of antibodies have been accomplished by removal of the Fc portion of the IgG. Generating smaller fragments has resulted in a decrease in the blood half-life from several days for the IgG to several hours. This rapid blood clearance has in turn been translated into more rapid diagnostic imaging of myocardial infarction, as well as other types of targets such as thrombi and tumors (17,18).

The single-chain antibody or sFv is a novel recombinant polypeptide composed of the antimyosin (R11D10) variable heavy chain amino acid sequence (V_H) joined to the variable light chain sequence (V_L). The carboxyl terminus of the V_H is linked by a 15-amino-acid peptide to the amino terminus of the V_L. Because only a small percent of the absolute dose is actually taken up at the infarct,

TABLE 2
Infarct Uptake

	Fab-DTPA	Fab'-RP-1	sFv-RP-1
Infarct-to-blood	6.3 ± 5.4	3.1 ± 1.2	$15.3 \pm 10.7^*$
Infarct-to-normal	19.6 ± 12.3	15.2 ± 5.4	$43.3 \pm 13.5^\dagger$
%ID/g infarct	0.0841 ± 0.0654	0.0481 ± 0.0110	0.0417 ± 0.0168

* $p < 0.05$ vs. Fab'-RP-1 and Fab-DTPA.
† $p < 0.01$ vs. Fab'-RP-1 and Fab-DTPA.
Radiolocalization indices and infarct uptake for fragments at 5 hr. Data represent ratios for cpm/g (mean ± s.d.) for Fab-DTPA (n = 8), Fab'-RP-1 (n = 4) and sFv-RP-1 (n = 4).

development of an agent that is more rapidly cleared from the blood, but at the expense of a reduction in affinity, would not be beneficial. Our results demonstrate that the sFv fragment maintained high immunoreactivity in vitro and in vivo. The rapid blood clearance of sFv is consistent with the observation that reduction in the relative molecular weights of the imaging agents results in faster blood clearance (IgG < F(ab')$_2$ < Fab or Fab'). Although the sFv cleared significantly faster than the other fragments, sFv maintained the same degree of infarct avidity as the larger Fab' and Fab molecules. The combined rapid clearance and high affinity of sFv resulted in superior infarct imaging. These results suggest that previous limits to early infarct visualization were, at least in part, caused by slow blood clearance rather than low infarct uptake.

Since ^{99m}Tc is the radionuclide of choice in nuclear medicine, it was chosen as the radiolabel for the sFv. We have previously reported (10) the development of a new ^{99m}Tc labeling method via an ester-linker, bifunctional chelator (RP-1) that allows the site-specific attachment of the chelator to the Fab' sulfhydryls. This chelator was designed to be metabolically cleaved from the protein, thereby producing a species which is readily excreted. Studies reported previously with ^{99m}Tc-Fab'-RP-1 and ^{111}In-Fab-DTPA antimyosin have shown they are equivalent in both blood clearance and infarct uptake. By evaluating the sFv in this manner, it is clear that differences in biodistribution and clearance kinetics are due to the sFv itself and not the RP-1 chelator.

Single-chain Fv proteins may offer advantages when compared to whole antibodies or Fab fragments. These advantages include more rapid blood clearance, potentially lower immunogenicity, lower retention in critical organs and better lesion penetration. Colcher et al. (17) have recently characterized the in vitro and in vivo properties of an iodinated sFv fragment derived from the genetic sequence of the variable regions of B6.2, an antitumor monoclonal antibody. Studies in mice indicated that the ^{125}I-sFv cleared approximately 3 to 5 times faster than the ^{131}I-Fab' fragment of B6.2. Comparison of blood clearance in mice between ^{99m}Tc-sFv-RP-1 and other fragments in the present study confirm a similar increase in the rate of blood clearance. Blood activity of ^{99m}Tc-sFv-RP-1 decreased by one-half between 15 min and 1 hr. This was in contrast to the clearance of the ^{125}I-sFv for B6.2, which seemed to plateau after 15 min. Further comparisons with B6.2 cannot be made because blood clearance was studied only up to 30 min for the B6.2 sFv, and the radiolabel was different.

In a similar study by Laroche et al. (9), a recombinant single-chain molecule containing the variable domains of a Mab specific for fragment D-dimer of human cross-linked fibrin was reported to clear significantly faster than the intact monoclonal. Results in nephrectomized rabbits resulted in a significant prolongation of the clearance, suggesting the clearance of the sFv occurs primarily via

the kidneys. Results for the ^{99m}Tc-sFv-RP-1 from murine biodistribution (Fig. 2), which showed the kidney to be the primary route of excretion, support these findings.

To further characterize the pharmacokinetics of antimyosin sFv, we studied the clearance in a canine model of acute myocardial infarction. Use of the dog enabled simultaneous evaluation of the time course of uptake of ^{99m}Tc-sFv-RP-1 in the infarct and blood clearance kinetics in the same animal. Our results are in agreement with previous reports that the blood half-life for ^{111}In-Fab-DTPA is between 2 and 3 hr. We also found that blood clearance for the ^{111}In-Fab-DTPA and ^{99m}Tc-Fab'-RP-1 are nearly identical. Therefore, ^{99m}Tc labeling of the Fab' fragment via RP-1 does not affect blood clearance. This implies that the four- to fivefold faster clearance of the sFv compared to the Fab' or Fab fragments is attributable to the fragment itself, and not the labeling method. This increase in blood clearance resulted in the more rapid imaging of a myocardial infarct.

A major concern in using a smaller protein for imaging is that the enhanced clearance would preclude maintenance of concentrations sufficient for adequate uptake. For example, studies with small peptides like RGD (arginine-glycine-aspartic acid) which have been shown to competitively inhibit the fibrinogen receptor on platelets (glycoprotein IIb/IIa), show that these small molecules are transiently effective only if they are delivered locally and at high concentration (20). However, our results indicate that the binding properties of antimyosin sFv do not differ significantly from either the Fab-DTPA or Fab'-RP-1. Clinical trials of the Fab-DTPA fragment of antimyosin have demonstrated that it is nonimmunogenic (3). Because of the smaller size of the antimyosin sFv molecule, the absence of immunogenicity would likewise be anticipated. However, clinical studies will be necessary to determine if the antimyosin sFv, which is produced in bacteria and includes a novel linker, results in an immune response in man.

The animal model employed in the investigation was one with a temporary coronary artery occlusion followed by reperfusion. Similar results have been obtained with ^{99m}Tc-pyrophosphate and ^{99m}Tc-glucaric acid under conditions of reperfusion (21). However, as is the case for antimyosin Fab-DTPA imaging of permanently occluded infarcts, significantly longer times (1 to 3 days) for accumulation of these agents are required. While we are undoubtedly in the age of reperfusion, it will be important to demonstrate the detection of myocardial necrosis with and without reperfusion, as many acute infarcts occur with coronary artery occlusion without reperfusion. Additional studies are required to investigate the affinity of this new sFv for necrosis under conditions of permanent occlusion.

Our results suggest that the genetically engineered sFv may have significant imaging advantages compared to currently available agents. One might expect that if an antimyosin sFv fragment successfully images myocardial

infarction, a process which requires the agent to diffuse and bind to its antigen extravascularly, that development of sFv fragments to intravascular antigens relevant to cardiovascular diseases may also have clinical utility in both therapeutic and diagnostic applications.

REFERENCES

1. Rosebrough SF, Grossman ZD, McAfee JG, et al. Thrombus imaging with indium-111 and iodine-131-labeled fibrin-specific monoclonal antibody and its F(ab')₂ and Fab fragments. *J Nucl Med* 1988;29:1212-1222.
2. Murray JL, Rosenblum MG, Lamki L, et al. Clinical parameters related to optimal tumor localization of indium-111-labeled mouse antimelanoma monoclonal antibody ZME-018. *J Nucl Med* 1987;28:25-33.
3. Brown JM, Dean RT, Kaplan P, et al. Absence of human antimouse (HAMA) response in patients given antimyosin Fab-DTPA monoclonal antibody [Abstract]. *J Nucl Med* 1988;29:851.
4. Reynolds JC, DelVecchio S, Sahakara H, et al. Anti-murine antibody response to mouse monoclonal antibodies: clinical findings and implications. *Int J Radiat Appl Instrum[B]* 1989;16:121-125.
5. Berger H, Lahiri A, Leppo J, et al. Antimyosin imaging in patients with ischemic chest pain: initial results of phase III multicenter trial [Abstract]. *J Nucl Med* 1988;29:805.
6. Khaw BA, Yasuda T, Gold HK, et al. Acute myocardial infarct imaging with indium-111-labeled monoclonal antimyosin Fab. *J Nucl Med* 1987;28:1671-1678.
7. Huston JS, Levinson D, Mudgett-Hunter M, et al. Protein engineering of antibody binding sites: recovery of specific activity in an anti-digoxin single-chain Fv analogue produced in *Escherichia coli*. *Proc Natl Acad Sci USA* 1988;85:5879-5883.
8. Bird RE, Hardman KD, Jacobson JW, et al. Single-chain antigen-binding proteins. *Science* 1988;242:423-426.
9. Laroche Y, Demaeyer M, Stassen JM, et al. Characterization of a recom-binant single-chain molecular comprising the variable domains of a monoclonal antibody specific for human fibrin fragment D-dimer. *J Biol Chem* 1991;266:16343-16349.
10. Weber RW, Boutin RH, Nedeman MA, Lister-James J, Dean RT. Enhanced kidney clearance with an ester-linked ⁹⁹ᵐTc-radiolabeled antibody Fab'-chelator conjugate. *Bioconjugate Chem* 1990;1:431-437.
11. Ellman GL. Tissue sulfhydryl groups *Arch Biochem Biopshy* 1959;82:70-77.
12. Schier JJ, Adelstein RS. Structural and enzymatic comparison of human cardiac muscle myosins isolated from infants, adults, and patients with hypertrophic cardiomyopathy. *J Clin Invest* 1982;69:816-825.
13. Beller GA, Khaw BA, Haber E, Smith TW. Localization of radiolabeled cardia myosin-specific antibody in myocardial infarcts. Comparison with technetium-99m stannous pyrophosphate. *Circulation* 1977;55:74-78.
14. OHL. *An introduction to statistical methods and data analysis*, 2nd edition. Boston, MA: PLUS Publishers; 1984:365-370.
15. SAS Institute Inc. *SAS/STAT users guide, version 6*, 4th edition, volume 2. Cary, NC: SAS Institute Inc.; 1989:1135-1193.
16. Khaw BA, Beller GA, Haber E, Smith TW. Localization of cardiac mysoin-specific antibody in myocardial infarction. *J Clin Invest* 1976;58:439-446.
17. Knight LC, Maurer AH, Ammar IA, et al. Tc-99m antifibrin Fab' fragments for imaging venous thrombi: evaluation in a canine model. *Radiology* 1989;173:163-169.
18. Pak KY, Nedelman MA, Fogler WE, et al. Evaluation of the 323/A3 monoclonal antibody and the use of technetium-99m-labeled 323/A3 Fab' for the detection of pan adenocarcinoma. *Nucl Med Biol* 1991;18:483-497.
19. Colcher D, Bird R, Roselli M, et al. In vivo tumor targeting of a recombinant single-chain antigen-binding protein. *J Natl Cancer Inst* 1990;82:1191-1197.
20. Yasuda T, Gold HK, Leinbach RC, et al. Kistrin, a polypeptide platelet GPIIb/IIIa receptor antagonist, enhances and sustans coronary arterial thrombolysis with recombinant tissue-type plasminogen activator in a canine preparation. *Circulation* 1991;83:1038-1047.
21. Willerson JT. Detection of acute myocardial infarcts by infart-avid imaging [Editorial]. *J Nucl Med* 1991;32:269-271.